

LATTICE DESIGN FOR 5MeV-125mA CW RFQ OPERATION IN THE LIPAc

Y. Shimosaki^{†,1}, A. Kasugai, K. Kondo, K. Sakamoto, M. Sugimoto, QST, Rokkasho, Japan
 P. Cara, IFMIF/EVEDA Project Team, Rokkasho, Japan
 D. Duglue, H. Dzitko, R. Heidinger, F4E, Garching, Germany
 N. Chauvin, CEA/Saclay, Gif-sur-Yvette, France
 L. Bellan, M. Comunian, E. Fagotti, A. Pisent, INFN-LNL, Legnaro, Italy
 B. Branas, C. Oliver, I. Podadera, CIEMAT, Madrid, Spain
 H. Kobayashi, K. Takayama, KEK, Tsukuba, Japan
¹also at KEK Tsukuba, Japan

Abstract

The installation and commissioning of the LIPAc are ongoing under the Broader Approach agreement, which is the prototype accelerator of the IFMIF for proof of principle and design. The deuteron beam will be accelerated by the RFQ linac from 100 keV to 5 MeV during the commissioning phase-B and by the SRF linac up to 9 MeV during the phase-C. The commissioning phase-B+ will be implemented between phase-B and C to complete the engineering validation of the RFQ linac before installing the SRF linac. The lattice for the deuteron beam of 5 MeV and 125 mA at the commissioning phase-B+ was designed.

INTRODUCTION

The International Fusion Materials Irradiation Facility (IFMIF) aims to provide an accelerator-based, D-Li neutron source to produce high energy neutrons for DEMO reactor materials qualification. The Linear IFMIF Prototype Accelerator (LIPAc) is the prototype accelerator of the IFMIF for proof of principle and design. The installation and commissioning of the LIPAc are ongoing under the Broader Approach agreement, concluded between the European Atomic Energy Community (Euratom), whose implementing agency is F4E, and Japan [1, 2].

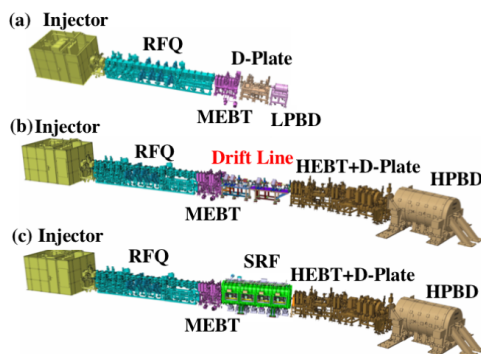


Figure 1: Accelerator components at (a) commissioning phase-B, (b) phase-B+, and (c) phase-C and D.

At the LIPAc, the deuteron beam (D+) of 140 mA generated from the injector will be accelerated by the RFQ linac from 100 keV to 5 MeV. During the commissioning

phase B, the D+ will be transported through the medium beam transport system (MEBT) and the beam diagnostic system (D-plate), and then it will be absorbed by the low power beam dump (LPBD) (see Fig.1(a)). It should be noted that, at the MEBT, there are 2 scrapers to remove the halo and 2 bunchers to match the longitudinal beam distribution to the SRF's one (see Fig. 2).

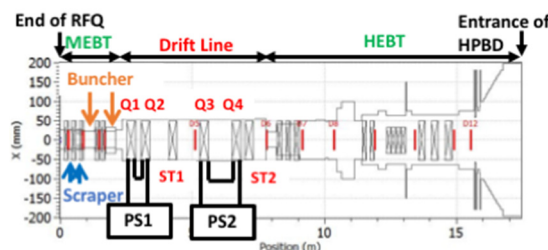


Figure 2: Schematic view of LIPAc at phase-B+.

The commissioning phase-B+ will be implemented between phase-B and C. Its main goal is to validate the CW operation of the RFQ linac on the condition of the D+ with 125 mA and 5 MeV for 30 minutes before installing the SRF linac. The phase-B+ consists of substituting the SRF linac in the phase-C configuration for a new beam transport line, which is called the drift line (see Figs. 1(b) and (c)). After passing through the drift line and the high energy beam transport system (HEBT) merged with the D-plate, the D+ will be absorbed by a high power beam dump (HPBD). During the phase-C, the D+ will additionally be accelerated by the SRF linac up to 9 MeV. The CW operation is not foreseen in phase-C, and it is foreseen in the phase-D whose accelerator components is identical with those of the phase-C.

In the new drift line at the Phase-B+, 4 quadrupole magnets, 2 steering magnets and 2 BPMs are assembled (Fig. 2). In order to meet the beam requirements for the phase-B+, the lattice design was performed. The beam requirements and results are presented in detail.

REQUIREMENTS FOR PHASE-B+

The requirements for the phase-B+ are listed as follows:

- The installation of the SRF linac is planned after the phase-B+, so that the installation and un-installation of the drift line must be simple. Therefore, it is planned that 4 quadrupole magnets are installed as the

[†]shimosaki.yoshito@qst.go.jp

Content from this work may be used under the terms of the CC BY 3.0 licence (© 2019). Any distribution of this work must maintain attribution to the author(s), title of the work, publisher, and DOI

combination of 2 doublets, which limits the length of the power cable and the number of the power supplies. In addition, 2 horizontally and vertically combined steering magnets are utilized at the drift line (Fig. 2).

- In order to safely install the SRF components after the operation of the phase-B+, the activation caused by the beam loss must be suppressed as much as possible.
- In order to avoid the damages of the HPBD from the radiation and heat stress caused by the absorbed D+, the following requirements must be satisfied at the entrance of the HPBD [3]: (1) The beam distribution should be as symmetrical as possible. (2) The beam power at the tail of the beam distribution should be suppressed to the reasonable level. (3) The divergence of the transverse rms beam size should be within $\pm 10 \sim 15 \%$ against the designed values which are -15.5 mrad in the horizontal and -17 mrad in the vertical.
- Since there is no SRF linac at the phase-B+, beam debunching occurs downstream the drift line. In order to obtain sufficient signal strength by the BPM pickups, the bunch length should be decreased as short as possible. So, the second buncher at the MEBT is utilized.
- In the phase-C, the D+ will be accelerated upto 9 MeV, so that the quadrupole magnets at the HEBT are originally tuned for the D+ of 9 MeV. In the phase-B+, however, there is no SRF acceleration. In the case of the high energy electron accelerators, the space charge is negligible so that the quadrupole fields can be normalized only by the beam momentum. But, at the LIPAc, the space charge effects become stronger as the beam energy is lower. Therefore, the retuned of the HEBT for the D+ of 5 MeV was performed.

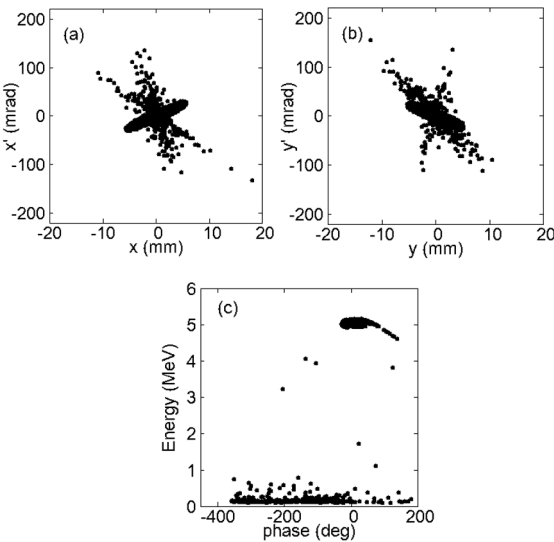


Figure 3: Initial beam distributions in (a) horizontal, (b) vertical and (c) longitudinal phase space, respectively.

SIMULATION RESULTS

For the lattice design, the simulation code TraceWin was used [4]. The beam distributions at the end of the RFQ evaluated by the INFN-LNL are shown in Figs. 3, which

were utilized as the initial beam distribution. The number of test particles in Figs. 3 is 898682. The halo particles shown in Figs. 3 were initially included in the initial beam, which are correspond to non-accelerated particles by the RFQ linac.

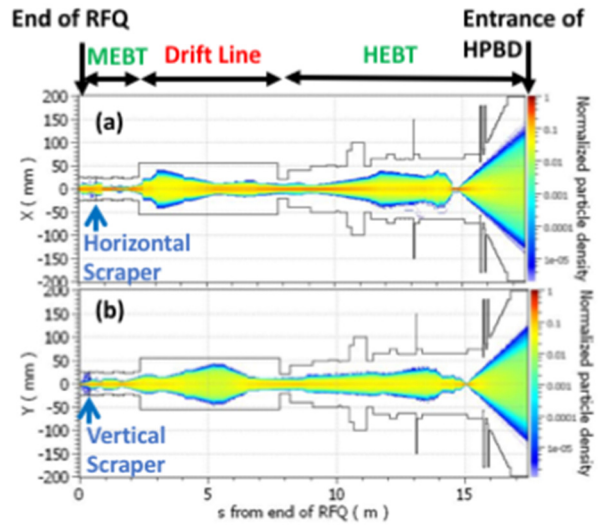


Figure 4: (a) Horizontal and (b) vertical beam densities.

The beam densities from the end of the RFQ linac to the entrance of the HPBD are shown in Figs. 4, and the beam distributions at the entrance of the HPBD are in Figs. 5, where the second buncher at the MEBT was set to 170 kV for shortening the bunch length.

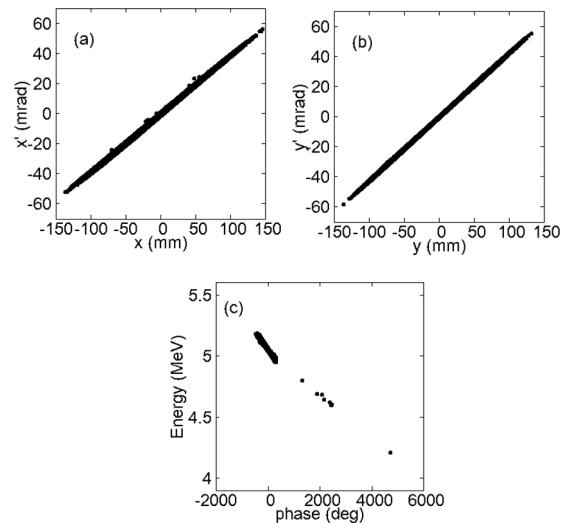


Figure 5: Beam distributions at entrance of HPBD in (a) horizontal, (b) vertical and (c) longitudinal phase space, respectively.

In order to relax the damages caused by the radiation and the heat stress, the transverse beam size is enlarged at the entrance of the HPBD (see Figs 4). The evaluated RMS sizes of the 6D phase space at the entrance of the HPBD are (39.5 mm, 15.6 mrad), (40.0 mm, 17.1 mrad) and (162.5 degree, 48.5 keV) in the horizontal, vertical and longitudinal direction, respectively. The transverse values satisfy the above requirements at the entrance of HPBD.

Table 1: Static and Dynamic Errors

Errors	Static	Dynamic
RFQ output displacement (mm)	± 0.1	
BPM accuracy (mm)	± 0.1	
MEBT and Drift Line		
Q displacement in x and y (mm)	± 0.2	± 0.02
Q gradient (%)		± 0.1
Q tilt in x and y (mrad)	± 10	± 1
Q tilt in z (mrad)	± 3	± 0.3
HEBT		
Q displacement in x and y (mm)	± 0.2	± 0.02
Q gradient (%)		± 0.1
Q tilt in x and y (mrad)	± 15.7	± 1.57
Q tilt in z (mrad)	± 5.2	± 0.52
B displacement in x and y (mm)	± 1.0	± 0.1
B tilt in x, y and z (mrad)	± 10.5	± 1.05
Buncher		
Buncher displacement in x and y (mm)	$\pm 1.0\text{mm}$	± 0.05
Buncher tilt in x and y (mrad)	± 29.7	± 5.06
Buncher field amplitude (%)	± 2.0	± 0.1
Buncher phase (mrad)	± 17.5	± 1.75

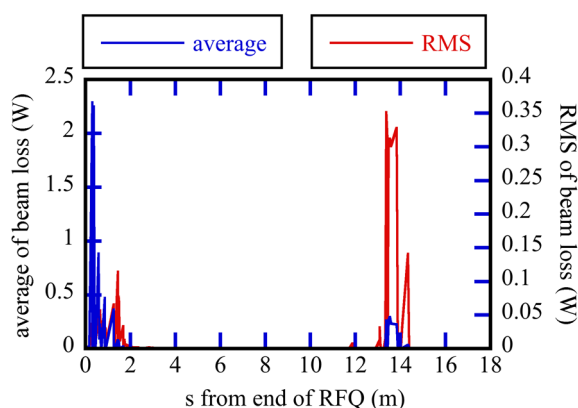


Figure 6: Beam loss distribution in case with errors.

In order to confirm the error tolerance, the 10000 linacs were surveyed with the static and dynamic errors listed in Table 1 [3, 5, 6]. The total number of tracked particles was 8986820000 and that of lost particles was 3910608 which is equivalent to 0.04 % beam loss. Fig. 6 shows the beam loss distribution with these errors, and the integrated energy distribution of the lost particles is shown in Fig. 7. The beam losses are mainly localized at the MEBT ($s = 0 \sim 2$

m in Figs. 6 and 7) and downstream area of the HEBT bending magnet ($s = 13 \sim 15$ m). Figure 6 indicates that the lost particles of less than 2 MeV are mainly localized around the MEBT scraper positions. It seems that these particles are lost not only due to the aperture limits of 2 scrapers but also by the chromatic effects at the MEBT because the beam losses are also observed after the position of the scrapers. The lost particles between 2 MeV and 5 MeV are also localized around the HEBT bending magnet because the orbits of these particles are significantly deviated from the designed orbit. In the error calculations, lost D^+ of more than 5 MeV, which could significantly cause the material activation [6], is however not observed.

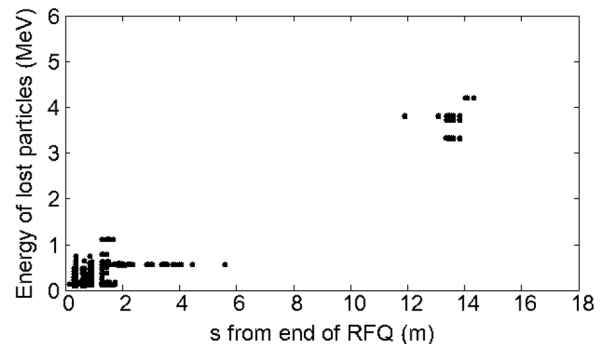


Figure 7: Integrated energy distribution of lost particles at 10000 linacs with errors.

SUMMARY AND FUTURE OUTLOOK

The commissioning phase-B+ will be implemented between phase-B and C to complete the engineering validation of the RFQ linac before installing the SRF linac. The quadrupole fields were optimized for the deuteron beam of 125 mA and 5 MeV to satisfy the beam requirements such as to suppress the beam loss to avoid the damage of the HPBD caused by the radiation and the heat stress, etc.

It is planned to install the drift line from September 2019 and to start the operation from February 2020.

REFERENCES

- [1] J. Knaster *et al.*, Nucl. Mater. Energy 9 (2016) 46.
- [2] J. Knaster, A. Moeslang, and T. Muroga, *Nature Physics* 12 (2016) 424.
- [3] F. Arranz *et al.*, “LIPAc HEBT Line and Beam Dump Engineering Design Report”, technical note, LIPAc EU-HT, 2012.
- [4] <http://irfu.cea.fr/Sacm/logiciels/index.php>
- [5] N. Chauvin *et al.*, “Start-to-end Beam Dynamics Simulations for the Prototype Accelerator of the IFMIF/EVEDA Project”, in *Proc. 2nd Int. Particle Accelerator Conf. (IPAC'11)*, San Sebastian, Spain, Sep. 2011, paper MOPS026, pp. 655-657.
- [6] P.A.P Nghiem *et al.* “Design report beam dynamics studies for the IFMIF-EVEDA accelerators”. Technical report, IFMIF-EVEDA-ASG-BD10-R006-A, 2010.